Absorbing-state phase transitions with extremal dynamics

Ronald Dickman* and Guilherme J. M. Garcia†
Departamento de Física, Instituto de Ciências Exatas, Universidade Federal de Minas Gerais, Caixa Postal 702, CEP 30123-970, Belo Horizonte-Minas Gerais, Brazil
(Received 11 October 2004; published 16 June 2005)

Extremal dynamics represents a path to self-organized criticality in which the order parameter is tuned to a value of zero. The order parameter is associated with a phase transition to an absorbing state. Given a process that exhibits a phase transition to an absorbing state, we define an "extremal absorbing" process, providing the link to the associated extremal (nonabsorbing) process. Stationary properties of the latter correspond to those at the absorbing-state phase transition in the former. Studying the absorbing version of an extremal dynamics model allows to determine certain critical exponents that are not otherwise accessible. In the case of the Bak-Sneppen (BS) model, the absorbing version is closely related to the "f-avalanche" introduced by Paczuski, Maslov, and Bak [Phys. Rev. E **53**, 414 (1996)], or, in spreading simulations to the "BS branching process" also studied by these authors. The corresponding nonextremal process belongs to the directed percolation universality class. We revisit the absorbing BS model, obtaining refined estimates for the threshold and critical exponents in one dimension. We also study an extremal version of the usual contact process, using mean-field theory and simulation. The extremal condition slows the spread of activity and modifies the critical behavior radically, defining an "extremal directed percolation" universality class of absorbing-state phase transitions. Asymmetric updating is a relevant perturbation for this class, even though it is irrelevant for the corresponding nonextremal class.

DOI: 10.1103/PhysRevE.71.066113 PACS number(s): 05.65.+b, 05.70.Jk, 05.40.−a, 05.70.Fh

I. INTRODUCTION

Extremal dynamics has been employed extensively in modelling far from equilibrium systems such as biological evolution [1] and driven interfaces [2,3]. Although processes with extremal dynamics do not have a phase transition (there is no control parameter) they exhibit scaling properties reminiscent of those observed at continuous phase transitions [4,5]. Indeed, it was suggested some time ago that the appearance of "self-organized" scaling properties in extremal dynamics and in sandpile models corresponds to forcing the order parameter (associated with an underlying phase transition) to zero from above [6]. The connection between extremal dynamics and directed percolation (DP), the prime example of an absorbing-state phase transition, was first suggested by Paczuski, Maslov, and Bak [4] and investigated in detail by these authors in the context of the Bak-Sneppen (BS) model and related processes [5]. (The latter work, as well as Ref. [7], clearly demonstrated that the critical exponents of the BS model are *not* those of DP.) Sornette and Dornic [8] and Grassberger and Zhang [9] have shown how a variant of directed percolation may be transformed via extremal dynamics to display SOC. These studies indicate that self-organized criticality (SOC) [10] under extremal dynamics arises because the system is driven to a critical point associated with a phase transition to an absorbing state [8], as is also the case for sandpiles [11].

The purpose of this work is to explore the connection between scale invariance under extremal dynamics and phase transitions to an absorbing state, in particular the transformation of a (nonextremal, non-SOC) model having an absorbing state to one exhibiting SOC under extremal dynamics. We develop a general scheme relating the two classes of models via an intermediate, "extremal-absorbing" process whose absorbing-state critical point corresponds exactly to the critical behavior observed in the corresponding SOC model. Two examples (the BS model and an extremal contact process) are studied in detail, yielding refined estimates for critical properties, and evidence of a universality class associated with absorbing phase transitions under extremal dynamics.

The prime example of extremal dynamics is the BS model [1,12], proposed to explain mass extinctions observed in the fossil record. While its application in the evolutionary context is debated [13], it remains an intriguing and incompletely understood example of scaling behavior far from equilibrium. The contact process (CP) [14] is the most familiar example of a Markov process exhibiting a phase transition to an absorbing state. We focus on the absorbing version of the BS model, and the extremal version of the CP, to illustrate the relations between extremal dynamics and absorbing phase transitions. Our analysis of the spread of activity leads to refined values for the exponents $\delta, \eta, \nu_{\|}, \beta'$, and z_{sp}, and for the critical threshold of the BS model. Finite-size scaling analysis of stationary properties at the critical point yields estimates of the exponent ratios $\beta/\nu_{\perp}$ and $\nu_{\|}/\nu_{\perp}$.

Studies of modified BS models have shown that scaling properties are insensitive to changes that preserve its basic symmetries (that is, invariance under translation and reflection) [15–17], pointing to the existence of a BS universality class. Nonextremal models that exhibit a phase transition to an absorbing state, and that possess these same symmetries,

*Electronic address: dickman@fisica.ufmg.br
†Electronic address: gjmg@fisica.ufmg.br

and no additional ones, belong generically to the directed percolation (DP) universality class [18,19]. Here we show that such models fall in a "extremal-DP" universality class when modified to follow extremal dynamics. Thus extremal dynamics is a relevant perturbation for absorbing-state transitions, just as was shown by Sneppen in the context of interface depinning [2].

The balance of this paper is organized as follows. Section II presents a general scheme linking ordinary absorbing-state phase transitions and extremal dynamics via an intermediary "extremal-absorbing" model. In Sec. III we describe our simulation results. Our findings regarding scaling and universality are discussed in Sec. IV. Mean-field analyses are presented in Appendix A, and an improved simulation algorithm in Appendix B.

II. ABSORBING STATE MODELS AND EXTREMAL DYNAMICS

In this section we examine how a stochastic model with an absorbing-state phase transition may be transformed to exhibit SOC under extremal dynamics. We begin, for generality, by defining a rather abstract scheme, and then discuss specific examples. A large class of models exhibiting an absorbing-state phase transition may be formulated as follows [20–23]. Consider a stochastic process $\mathcal{S}$ defined on a connected graph $\mathcal{G}$ of N sites. ($\mathcal{G}$ consists of a set of sites with links between certain pairs of sites. Typical examples are a ring of N sites, and the d-dimensional hypercubic lattice $\mathbb{Z}^d$, with links between nearest neighbors.) The *state* $\sigma(i)$ of site i is 0 or 1, the latter value denoting an active site, the former an inactive one. For each site i in $\mathcal{G}$ we define a neighborhood $v(i) \subset \mathcal{G}$, or, more generally, a set of neighborhoods $v_1(i), v_2(i), \ldots, v_n(i)$.

The dynamics of $\mathcal{S}$ proceeds in steps. Each step involves choosing an active site i (the *central site* for this step), at random, and changing the states of the sites in $v(i)$ according to a certain rule f. In case there are two or more neighborhoods, one of them, $v_r(i)$ say, is chosen at random from the collection, with probability p_r, and a rule f_r is applied to the site or sites in v_r. In general f (or f_r) is a probabilistic rule. At each step the number of active sites may change, and if at any moment there are no active sites [$\sigma(i)=0$, $\forall i \in \mathcal{G}$], the process has fallen into an absorbing state and there is no further evolution. Otherwise the dynamics proceeds to the next step.

Using σ_n to denote the entire set of activity variables $\sigma(1), \sigma(2), \ldots, \sigma(N)$ at step n, the dynamics generates a sequence $\sigma_1, \sigma_2, \ldots$ starting from the initial configuration σ_0. It is frequently of interest to associate a continuous time variable t with the process. This is usually done by associating a time increment $\Delta t = 1/N_a$ with each step, where N_a is the number of active sites just before the step is realized. We define the *order parameter* as $\rho(t) = \mathrm{Prob}[\sigma_t(i)=1]$, i.e., the fraction of active sites at time t. (The event space here is the set of all realizations of the process up to time t, starting from a given initial probability distribution on configuration space.) If the stationary order parameter, defined by $\lim_{t\to\infty}\lim_{N\to\infty}\rho$, vanishes, the process is said to be in the *absorbing phase*; otherwise it is in the *active* phase.

A simple model exhibiting a phase transition to an absorbing state is the *contact process* [14]. Here we consider the one-dimensional version. There are three sets $v_r(i)$, conveniently denoted as $v_0(i)=i$ and $v_\pm(i)=i\pm1$, with associated probabilitites p_0 and $p_\pm=(1-p_0)/2$. In terms of the usual parametrization [14,23], $p_0=1/(1+\lambda)$, where $\lambda \geqslant 0$ represents the rate of spread of activity. (In the "epidemic" interpretation of the CP, active sites represent infected organisms, inactive sites susceptibles, and λ is the infection rate.) The updating rules are $f_0=0$, $f_\pm=1$. In other words, an active site has a probability per unit time of $1/(1+\lambda)$ to become inactive, while an inactive site j becomes active at rate $\lambda n_a(j)/[2(1+\lambda)]$, where $n_a(j)$ is the number of active neighbors of site j. The one-dimensional CP exhibits a continuous phase transition between an absorbing phase and an active one at $\lambda_c \simeq 3.297\,85$ [20,22,23].

It is convenient to associate the control parameter with the updating rule f rather than with the probabilities p_r. We therefore reformulate the CP as follows. With the sets $v_0(i)$ and $v_\pm(i)$ defined above, we take $p_0=1/2$ and $p_\pm=1/4$, and define $q=\lambda/(1+\lambda)$. The updating functions are

$$f_0 = \begin{cases} 1, & \text{w.p.} \quad q, \\ 0, & \text{w.p.} \quad 1-q \end{cases} \tag{1}$$

('w.p.' denotes "with probability"), and

$$f_\pm = \begin{cases} 1, & \text{if } \sigma(i\pm1)=1 \\ 1, \text{w.p. } q & \text{if } \sigma(i\pm1)=0. \\ 0, \text{w.p. } 1-q & \end{cases} \tag{2}$$

It is easy to verify that the transition rates satisfy $w(0\to1)/w(1\to0)=n_a\lambda/2$, just as in the original formulation. The critical value $q_c \simeq 0.767\,33$.

The following three-site contact process (CP3) will play an important role in our analysis [24]. For each site we define the set $v(i)=\{i-1,i,i+1\}$ (the central site and its nearest neighbors). The updating function f takes values of 1 and 0 with probabilities q and $1-q$ respectively, independently at each of the three sites in $v(i)$. (In Ref. [24] this is called model 3.) Simulations of the CP3 show that it exhibits a continuous phase transition at $q=q_c \simeq 0.635\,23(3)$.

We shall assume that the process $\mathcal{S}$ is defined so that the control parameters (such as q) are associated with the updating rule f. Each time a site is updated, the value of f may be determined by comparing a random number x with the parameter in question. (This is of course the usual procedure in simulations.) In the CP3, for example, we take $f=1$ if $x<q$, and zero otherwise, where x is uniformly distributed on the interval [0,1]. Call the random number associated with the most recent updating of site i, x_i, so that $\sigma(i)=\Theta(q-x_i)$ with Θ the unit step function. **(**The initial values of the x_i are assigned according to the state variables $\sigma(i)$. For example, if all sites are initially active, we draw the initial x_i from the distribution uniform on $[0,q]$.**)** For the CP, Eq. (1) requires that we update the central site i with a number chosen uniformly from [0,1]. According to Eq. (2), the same applies

when updating an *inactive* neighbor ($i\pm1$), but when updating an *active* neighbor, the random number x is drawn from the interval $[0,q]$, since an active neighbor remains active.

Summarizing, we have shown how a stochastic process $\mathcal{S}$ may be formulated using a set of random variables x_i, such that site i is active if x_i is smaller than a certain parameter q. $\mathcal{S}$ suffers an absorbing-state phase transition at $q=q_c$. We now define two related processes, $\mathcal{S}_{EA}$ and $\mathcal{S}_E$. The former, *extremal absorbing* process, is obtained by taking the central site as *the active site having the smallest* x_i, rather than choosing it at random from among the currently active sites. As in the original process $\mathcal{S}$, if there are no active sites (i.e., $x_j>q$, $\forall j\in\mathcal{G}$), the process has reached an absorbing configuration and the evolution ceases. Thus $\mathcal{S}_{EA}$ possesses an absorbing state, and since the original process $\mathcal{S}$ exhibits a phase transition between an active and an absorbing phase as the control parameter q is varied, we expect $\mathcal{S}_{EA}$ to as well, at some value $q_{c,E}$. (The reason is that the relative likelihood of generating and destroying active sites varies with q, just as in $\mathcal{S}$.) Mean-field theory (see Appendix A) yields $q_{c,E}=q_c$. Due to the different correlations generated under extremal dynamics, however, the critical value $q_{c,E}$ of $\mathcal{S}_{EA}$ is in general different from q_c.

We define the *extremal* process $\mathcal{S}_E$ by relaxing the condition in $\mathcal{S}_{EA}$, that the extremal site i must be active (i.e., have $x_i<q$) for the dynamics to proceed. If $\mathcal{S}$ is the original contact process, then $\mathcal{S}_E$ is a process in which either the minimal site or one of its nearest neighbors is updated at each step. If $\mathcal{S}$ is the CP3, $\mathcal{S}_E$ is the familiar Bak-Sneppen model. Note that $\mathcal{S}_E$ has no absorbing state, hence no phase transition to such a state. Its stationary properties are nevertheless intimately connected with the critical-point properties of $\mathcal{S}_{EA}$.

Of particular interest is the stationary probability density $\overline{p}(x)$ of site variables under extremal dynamics. In the Bak-Sneppen model, as is well known, the density is a step function, $\overline{p}(x)=C\Theta(x-q_{c,E})\Theta(1-x)$, in the infinite-size limit. [$C=1/(1-q_{c,E})$ is the normalization factor.] We expect $\overline{p}(x)$ to exhibit a step-function singularity in any extremal model $\mathcal{S}_E$ [15]. This feature is in fact already present in the original model $\mathcal{S}$ at its critical point, because at the critical point $q=q_c$, the stationary density of active sites (having $x_j<q$) tends to zero as the system size N goes to infinity. The distribution on the "allowed" region $x>q$ is uniform, since the x_j are drawn from a uniform distribution. Thus $\overline{p}(x)$ jumps from zero to a finite value at $x=q_c$. In the *supercritical* regime ($q>q_c$), $\overline{p}(x)$ is equal to a constant p_1 for $x<q$, so that $qp_1=\rho$ (the order parameter), and takes a different constant value, p_2, on the interval $[q,1]$. Once again, the stationary density is discontinuous at $x=q$.

What holds for $\mathcal{S}$ also holds qualitatively for $\mathcal{S}_{EA}$. The critical value $q_{c,E}$ may, as noted, differ from q_c, but since $\mathcal{S}_{EA}$ exhibits an absorbing-state phase transition, its stationary distribution $\overline{p}(x)$ also has a step-function singularity. Just at $q=q_{c,E}$, the order parameter $\rho=0$, but as $N\to\infty$ the survival time of the process tends to infinity. This means that the process can survive indefinitely, with the choice of the central site *restricted to the set having* $x\leqslant q_{c,E}$. The presence of active sites in the range $q_{c,E}<x\leqslant q$ is then irrelevant, since a site with $x\leqslant q_{c,E}$ is always available. Thus for $q\geqslant q_{c,E}$, the distribution $\overline{p}(x)$ exhibits a step-function singularity at $q_{c,E}$. Extremal dynamics effectively "pins" the singularity at $q_{c,E}$. The foregoing remarks on $\mathcal{S}_{EA}$ obtain in the infinite-size limit; for finite N there is a nonzero probability (for $q<1$), that all sites have $x>q$ so that the system eventually becomes trapped in the absorbing state. (The mean lifetime, however, is expected to grow exponentially with N, for $q>q_{c,E}$.)

In summary, if $\mathcal{S}$ exhibits an absorbing-state phase transition, then $\mathcal{S}_{EA}$ should as well, although not necessarily at the same value of q. The distribution $\overline{p}(x)$ possesses a step function singularity in both cases. Near the critical point ($q\gtrsim q_c$) of the original process $\mathcal{S}$ we expect $\rho\sim(q-q_c)^\beta$, with β the critical exponent associated with the order parameter. Below the upper critical dimension ($d_c=4$ for DP [18,19]), $\beta<1$. In the supercritical regime of $\mathcal{S}_{EA}$, on the other hand, $\rho=\int_0^q\overline{p}(x)dx\propto(q-q_{c,E})$ since $\overline{p}(x)$ jumps from zero to a finite value at $x=q_{c,E}$. Thus the order parameter exponent β is *unity* in $\mathcal{S}_{EA}$.

In $\mathcal{S}_E$, the central site is always chosen (in the $N\to\infty$ limit) from the set $\{i:x_i\leqslant q_{c,E}\}$, just as in $\mathcal{S}_{EA}$ at its critical point. Since the order parameter is zero in the latter case, we may assert that extremal dynamics effectively tunes the order parameter to zero. (ρ approaches zero from above as $N\to\infty$.) As we have seen, the existence of sites with $q_{c,E}<x<q$ becomes irrelevant in $\mathcal{S}_{EA}$, in the infinite-size limit. In other words, $\mathcal{S}_E$ is identical to the critical process $\mathcal{S}_{EA}$ in this limit. (Starting from the same initial configuration, and using the same set of random numbers, the same sequence of sites will be updated in the two processes.)

Since the extremal version of the CP3 is the familiar Bak-Sneppen model, we shall refer to the $\mathrm{CP3}_{EA}$ as the *absorbing Bak-Sneppen* (ABS) model. Our objective is to characterize the behavior of the ABS model and of the extremal and EA versions of the contact process. The ABS model is closely related to the *f-avalanche* process studied in Ref. [5]. An f-avalanche (in the present notation, q-avalanche), begins when the minimal site variable $x_{\min}<q$, the minimum having been *greater* than q at the preceding step or steps, and continues until the minimum is once again $>q$. (As q approaches $q_{c,E}$ from below, the mean avalanche duration diverges.) The dynamics of the BS model continues, regardless of whether a given avalanche has terminated or not. But in the ABS model $x_{\min}>q$ represents an absorbing state and the dynamics ceases. In the BS model, it is common to analyze the properties of q-avalanches in the stationary state. It is similarly of interest to study stationary properties of the ABS model, attained once the system has relaxed, after an initial transient period. We may also study the mean lifetime of the active state as a function of system size. Another approach to studying absorbing-state phase transitions consists in following the spread of activity starting from a single active site. This spreading phenomenon in the BS model was studied in Refs. [4,5], where it is called the BS branching process, and in Ref. [7] under the name of the BS($\tilde{p}$) model.

The assertions regarding extremal and extremal-absorbing models are supported by mean-field theory (MFT), as discussed in Appendix A. In particular, for the ABS model $\overline{p}=\frac{3}{2}\Theta(x-\frac{1}{3})$, just as in the MFT of the original BS model. In

the extremal and the extremal-absorbing contact process, the stationary probability densities exhibit (for $q > q_{c,E} = 1/2$), *two* discontinuities, one at $x = \kappa \equiv q^2/(3q-1)$, the other at $x = q > \kappa$. [These coalesce at $q = 1/2$. Note that the parameter q continues to influence the form of $\overline{p}$ in the extremal contact process, due to the nature of the updating rule, Eqs. (1) and (2).] These predictions are in qualitative agreement with simulation.

In the following section we report our simulation results. Although many models are considered, they may be organized as follows: absorbing, nonextremal (CP3); extremal-absorbing (ABS and CP_{EA}); extremal (CP_E). In some cases anisotropic versions are also considered.

III. SIMULATION RESULTS

A. Absorbing Bak-Sneppen model: Stationary properties

Taking advantage of the fact that the minimal site is almost always $\leqslant q_{c,E}$, we have devised a highly efficient simulation algorithm, as described in Appendix B. Using this method, we conducted extensive studies of the one-dimensional ABS model. We initialize the system with all sites active and allow it to relax until mean properties fluctuate about stationary values. Stationary properties are obtained from temporal averages over the set of surviving realizations. Each step corresponds to a time interval of $\Delta t = 1/N_a$, with N_a the number of active sites just before the updating is performed. Results for the stationary order parameter (i.e., the density of sites with $x < q$), confirm that in the supercritical regime ($q > q_{c,E}$), the order parameter grows linearly with $q - q_{c,E}$, as anticipated in Sec. II.

We study the finite-size scaling behavior of the stationary order parameter $\overline{\rho}$ and of the lifetime τ at the critical point. [τ is obtained from an exponential fit to the survival probability $P_s(t)$.] The expected finite-size scaling behaviors at the critical point are $\overline{\rho} \sim L^{-\beta/\nu_\perp}$ and $\tau \sim L^{\nu_\parallel/\nu_\perp}$. We performed simulations at $q = 0.667\,01$ and $0.667\,02$, the latter being the preferred literature value for the threshold in the one-dimensional BS model, while the former is favored by the results discussed in the following section. We studied systems of 1000, 2000, 4000, …, 32 000 sites in simulations of 2×10^7 to 3×10^8 time steps.

For $L = 4000$–$32\,000$, the results for the order parameter follow a power law with $\beta/\nu_\perp = 0.755(5)$. The data for smaller system sizes, however, show systematic deviations from a pure power law, leading us to seek a correction to scaling term; a correction decaying $\propto L^{-1/2}$ leads to a good fit. We fit the expression

$$\ln \overline{\rho} = -\frac{\beta}{\nu_\perp} \ln L - \frac{b}{L^{1/2}} \tag{3}$$

to the data for $L \geqslant 1000$, allowing $\beta/\nu_\perp$ and b as adjustable parameters; the best-fit values are $\beta/\nu_\perp = 0.769(7)$ and $b = 3.69(20)$. The simulation data, and the difference from best fit of Eq. (3) are plotted in Fig. 1, showing the high quality of fit. The data for the lifetime, using system sizes of 125, 250, …,8000 yield $\nu_\parallel/\nu_\perp = 2.12(1)$, with no obvious correction term (see Fig. 2). We also determined the stationary moment ratio $m = \overline{\rho^2}/\overline{\rho}^2$ at the critical point. The estimates for m decrease slowly with L, and appear, when plotted versus $L^{-0.25}$, to approach a limiting ($L \to \infty$) value of 1.030(5) (see Fig. 3). (For the one-dimensional CP, $m = 1.1737$ at the critical point.) Essentially the same results are obtained for $q = 0.667\,01$ and $0.667\,02$.

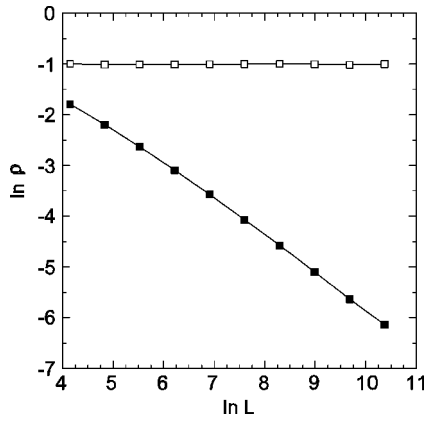

FIG. 1. Stationary activity density (filled symbols) $\overline{\rho}$ versus system size L in the one-dimensional ABS model at the critical point. Open symbols, difference between $\overline{\rho}$ and the fitting function, Eq. (3), shifted vertically for visibility.

B. Absorbing Bak-Sneppen model: Spread of activity

Scaling properties at an absorbing state phase transition are also reflected in the spread of activity from an initially localized region [28]. In spreading simulations of the ABS model we start the system with a single site $x_0 < q$ and all others above this value. (This is completely equivalent to the BS branching process studied in Refs. [4,5,7].) At $q = q_{c,E}$, the process generates a scale-invariant pattern of activity that may be characterized by power laws for the survival probability $P_s(t)$, the mean number of active sites $n(t)$ and the mean-square distance $R^2(t) = [n(t)]^{-1} \langle \Sigma_j r_j^2(t) \rangle$. [$r_j(t)$ denotes the position of the jth active site at time t. Note that $n(t)$ is

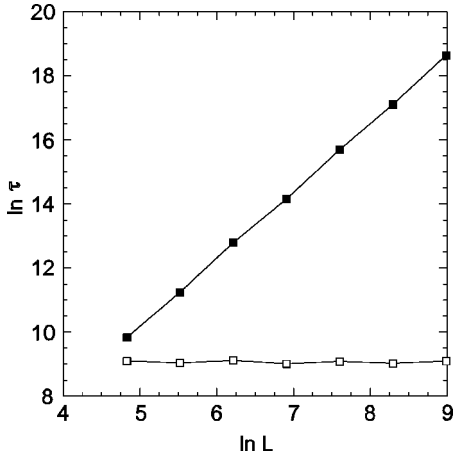

FIG. 2. Mean lifetime τ (filled symbols) versus system size L in the one-dimensional ABS model at the critical point. Open symbols, $\tau/L^{\nu_\parallel/\nu_\perp}$ (shifted vertically for visibility).

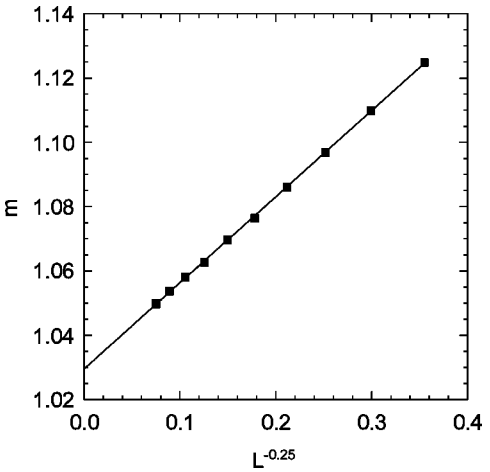

FIG. 3. Moment ratio m for the ABS model versus system size $L^{-0.25}$. Points, simulation data; line, best linear fit, $m=1.0295+0.268L^{-0.25}$.

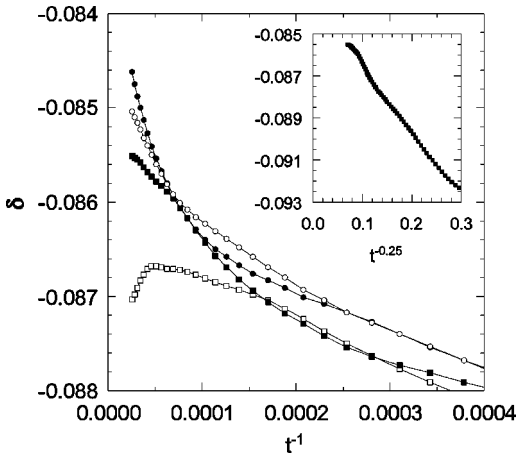

FIG. 4. Local slope $\delta(t)$ versus $1/t$ in the ABS model. q values (bottom to top) 0.667 00, 0.667 01, 0.667 02, and 0.667 03. Inset, data for $q=0.667\,01$ plotted versus $1/t^{0.25}$.

taken over all realizations, including those that have become trapped in the absorbing state at or before time t.] The scaling laws are typically written in the form

$$P_s \sim t^{-\delta}, \quad n \sim t^{\eta}, \quad R^2 \sim t^{z_{sp}}, \tag{4}$$

relations that have been verified to high precision for various examples [21,23]. (We use z_{sp} to denote the spreading exponent, to avoid confusion with the *dynamical* exponent z.) The appearance of power laws is commonly used to locate the critical point [23].

The spreading exponent δ is related to the avalanche size exponent τ, defined (in the BS model) via $P_D(s)\sim s^{-\tau}$, where $P_D(s)ds$ is the probability of an avalanche having a duration between s and $s+ds$. Thus the survival probability $P_s(t)=\int_t^\infty P_D(s)ds$, implying $\tau=1+\delta$.

We performed spreading simulations of the ABS model at $q=0.666\,99$, $0.667\,00$, $0.667\,01$, $0.667\,02$, and $0.667\,03$. Each realization was followed up to a maximum time of about 2.7×10^5; the total number of realizations ranged from 4×10^5 to 1.6×10^6, depending on the value of q. To locate the critical point we plot the local slope $\delta(t)=d\ln P/d\ln t$, versus t^{-1}. For $q<q_c$ the local slope is expected to veer downward at large times, and vice versa. [Numerically, $\delta(t)$ is given by the slope of a least-squares linear fit to the data in an interval $[t_0,20t_0]$, with geometric mean t.] On the basis of the local slope data (see Fig. 4) we conclude that $q_{c,E}=0.667\,01(1)$. This is consistent with previous estimates, which place the threshold at 0.667 02(8) [7] and 0.667 02(3) [5]. [We did not find analyses of the local slopes $\eta(t)$ or $z_{sp}(t)$, defined analogously to $\delta(t)$, useful in locating the critical point.]

Analyzing the data at the critical point, we are unable to obtain good fits to P_s, n, and R^2 using simple power-law expressions. Including a subdominant power-law correction in the relations of Eq. (4) greatly improves the quality of fit. In particular, the survival probability can be fit quite accurately using

$$\ln P_s \simeq -\delta\ln t + \phi_P t^{-1/4} + C, \tag{5}$$

where C is a constant and the best-fit values are $\delta=0.084(1)$ and $\phi_P=0.115$. The same value for δ is found using the data for $q=0.667\,02$. [The choice of a correction term decaying as $t^{-1/4}$ is motivated by the fact that the local slopes $\delta(t)$ and $z_{sp}(t)$ are essentially linear when plotted versus $t^{-1/4}$, as seen in the inset of Fig. 4.] In Fig. 5 we plot P_s and the ratio of P_s to the fitting function, Eq. (5); the ratio is seen to be essentially constant for $t>50$. The mean-square displacement may also be fit using an asymptotic power law and correction term. We find

$$\ln R^2 \simeq z_{sp}\ln t - \phi_R t^{-1/4} + C', \tag{6}$$

with $z_{sp}=0.921(10)$ and $\phi_R=1.703$.

It has been argued that $\eta=0$ quite generally for extremal dynamics [5,25]. Our data for the one-dimensional ABS model support this conclusion, on a double-logarithmic plot, $n(t)$ clearly grows more slowly than a power law. While η

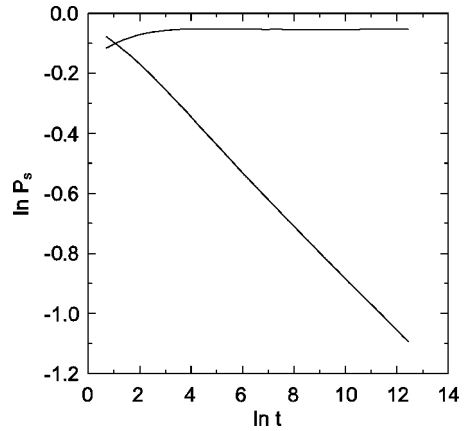

FIG. 5. Survival probability $P_s(t)$ in the ABS model at the critical point, $q=0.667\,01$. The nearly constant function represents the ratio of P_s to the fitting function, Eq. (5).

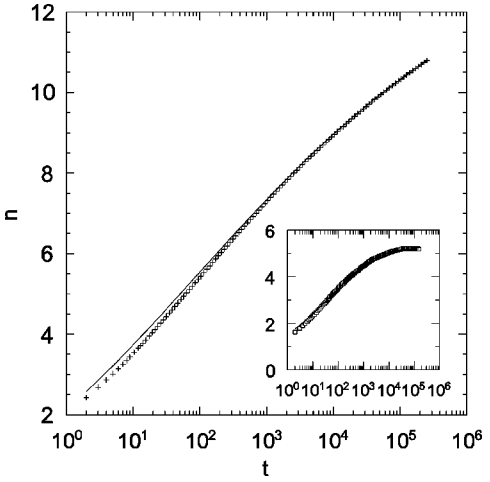

FIG. 6. Mean number of active sites $n(t)$ in the ABS model at the critical point, $q=0.667\,01$. The solid curve represents the fitting function described in the text. Inset, a similar plot, for the critical *anisotropic* ABS model.

$=0$ is compatible with $n(t)$ growing without limit as $t\to\infty$ [for example, $\propto(\ln t)^{\phi}$, as suggested in Ref. [7]], our results support the conclusion that $n(t)$ saturates at a *finite value* n_∞ at long times. Specifically, we are unable to fit the long-time behavior using an expression of the form $n\sim(\ln t)^{\phi}$. On the other hand, we find $d\ln n/d\ln t\propto t^{-\omega}$, with $\omega\simeq 0.149$, suggesting that $n(t)\simeq n_\infty\exp(-ct^{-\omega})$. In fact an excellent fit is obtained using $c=1.92$ and $n_\infty=14.574$, as can be seen in Fig. 6. [Saturation of $n(t)$ does not occur on the time scale of the simulation; for the anistropic case, shown in the inset of Fig. 6, saturation is in fact evident.]

In the absorbing phase ($q<q_{c,E}$), the survival probability must vanish as $t\to\infty$. Our data follow $P_s\sim t^{-\delta}e^{-t/\tau}$, where $\tau\sim|q-q_{c,E}|^{-\nu_\parallel}$, with $\nu_\parallel=2.54(2)$. On the other hand, for $q>q_{c,E}$, the survival probability tends to a finite value as $t\to\infty$. We obtain $\lim_{t\to\infty}P_s\equiv P_\infty\sim(q-q_{c,E})^{\beta'}$, with $\beta'=0.20(1)$. (In DP and allied models $\beta'=\beta$ [28], but this need not hold for models in other universality classes.) Our results for the critical exponents of the ABS model are summarized and compared with those for the contact process in Table I.

In the CP and other nonextremal models, the spread of activity in the *supercritical* regime follows a simple pattern: the size R of the active region grows linearly with time, and the number of active sites n grows $\propto t^d$. Our observation of subdiffusive spreading at the critical point motivates us to investigate spreading in the supercritical ABS model. We find that spreading is indeed *sublinear*. For example, using $q=0.75$ in a study extending to $t\simeq 2\times10^6$ to avoid transient effects, we obtain $R^2\sim t^{\chi}$ with $\chi=1.32(1)$ and $n\sim t^{\lambda}$ with $\lambda=0.66(1)$. (The exponent governing R^2 should be twice that for n, since active regions have a finite activity density in the supercritical regime.) Similar exponents are found for $q=0.70$ and 0.78. Once again, extremal dynamics slows the growth of activity.

TABLE I. Critical exponents for the one-dimensional absorbing Bak-Sneppen model (ABS) and contact process (CP). CP exponents from Refs. [23,40].

Exponent	ABS	CP
β	1	0.27649(4)
β'	0.20(1)	$(=\beta)$
$\nu_\parallel$	2.54(2)	1.73383(3)
$\beta/\nu_\perp$	0.77(1)	0.25208(5)
$\nu_\parallel/\nu_\perp$	2.12(1)	1.58071(11)
δ	0.084(1)	0.15947(3)
η	0	0.31368(4)
z_{sp}	0.921(10)	1.26523(3)

TABLE II. Spreading exponents for the CP3 and CP_{EA} models and the anisotropic absorbing Bak-Sneppen (AABS) model in one dimension.

Exponent	CP3	CP_{EA}	AABS
δ	0.162(2)	0.0855(20)	0.234(5)
η	0.312(2)	0	0
z_{sp}	1.265(4)	0.932(20)	1.425(10)

C. CP3 model

We performed spreading simulations of the CP3 model, using the approach described in the preceding section. Each realization is followed up to a maximum time of 6×10^4. Using power-law behavior of $P_s(t)$ and $n(t)$ as the criterion for criticality, we find $q_c=0.635\,25(3)$ for the CP3. (Note that this is some 5% smaller than the critical value of the corresponding extremal model.) Analyzing the local slopes, we obtain $\delta=0.162(2)$, $\eta=0.312(2)$, and $z_{sp}=1.265(4)$. These values are fully consistent with those for directed percolation (see Table II), confirming that the CP3 model belongs to the same universality class as the original contact process.

A striking difference between extremal and nonextremal models with an absorbing state is that the spread of activity in the critical process is much slower in the former. This is of course reflected in the value $\eta=0$ for extremal models (while, for example, $\eta=0.314$ for DP in one dimension), and in the subdiffusive growth in R^2 in the ABS model. In Figs. 7 and 8 we compare typical evolutions in the ABS model and its nonextremal analog, the CP3, at their respective critical points. It is evident that the activity spreads much more slowly in the ABS than in the CP3. A further notable difference is that in the ABS a site can remain active for a very long time, i.e., while it is not the minimum site or a neighbor of it. Thus the rates of both addition and loss of active sites are much smaller in the critical extremal process than in the corresponding nonextremal one.

D. Extremal CP

In light of the discussion of Sec. II, it is of interest to study the behavior of other absorbing-state models under extremal dynamics. As a first step we report simulation results

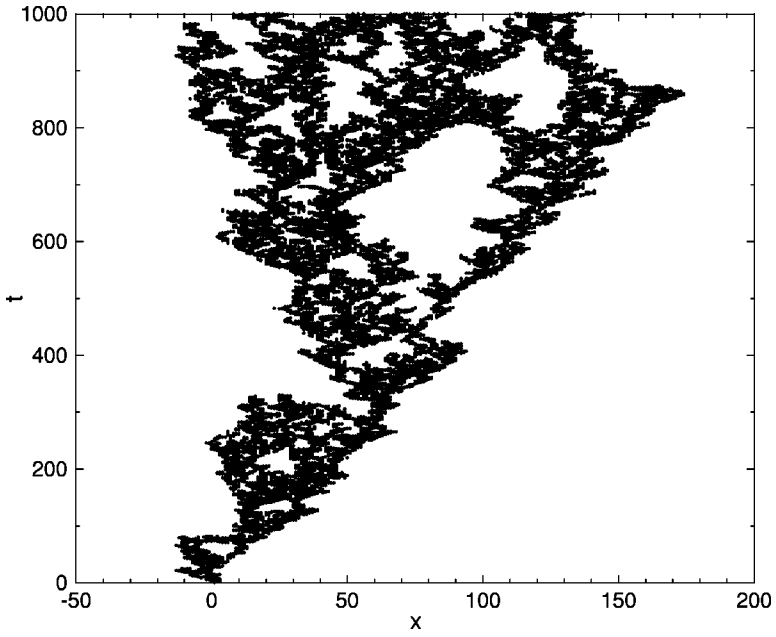

FIG. 7. Spread of activity in a typical realization of the critical CP3 model ($q=0.635\,25$).

for the extremal-absorbing contact process (CP_{EA}). We performed spreading simulations to determine $q_{c,E}$ and the exponents δ, η, and z_{sp}, using simulations running to a maximum time of 6×10^4 in 5×10^5 independent realizations. We find $q_{c,E}=0.794\,15(5)$ for the extremal CP, compared with 0.767 33 for the original (nonextremal) process. (Note that, as in the comparison between the CP3 and ABS models, $q_{c,E}>q_c$.)

As in the case of the ABS model, the decay of the survival probability at the critical point follows an expression of the form of Eq. (5), here with best-fit parameters $\delta=0.0855$ and $\phi_P=0.226$. The exponent δ is essentially the same as found for the ABS model, while the correction term is about twice as large. At the critical point the derivative $d\ln n/d\ln t \sim t^{-0.1}$, again indicating a behavior of the form $n(t) \simeq n_\infty \exp(-ct^{-\omega})$, here with $\omega=0.1$. The mean-square distance of active sites from the origin grows in a manner similar to that in the ABS model. We are again able to fit the data for R^2 using an expression of the form of Eq. (6), with $z_{sp}=0.932$ and $\phi_{R^2}=2.026$. These results strongly suggest that the CP_{EA} belongs to the same universality class as the ABS model.

We turn now to the rather surprising behavior of the stationary probability density $\overline{p}(x)$ in the extremal CP. Recall that mean-field theory (Appendix A) predicts $\overline{p}(x)=2\Theta(x-1/2)$ for $q<q_{c,E}=1/2$, while for $q>1/2$ there are two steps, one at $x=\kappa\equiv q^2/(3q-1)$, the other at $x=q$. In simulations of the CP_E on a ring we find a single step discontinuity for $q<q_{c,E}=0.794\,15$, and, for $q>q_{c,E}$, a pair of steps, one at $x=q$, the other at $x=q_s<q$. The positions of the singularities as obtained in simulation (using data for system sizes $L=100,\ 200,\ \ldots,\ 1600$ to extrapolate the position in the

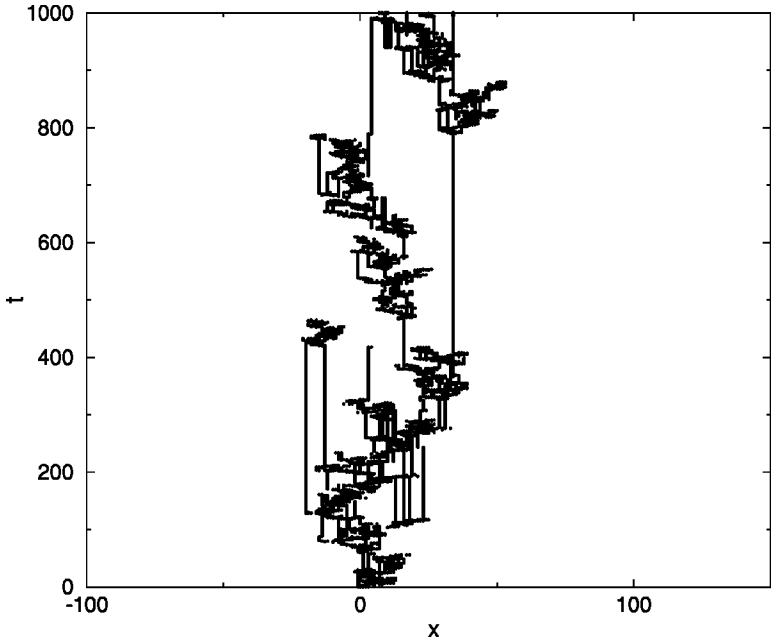

FIG. 8. Spread of activity in a typical realization of the critical ABS model ($q=0.667\,01$).

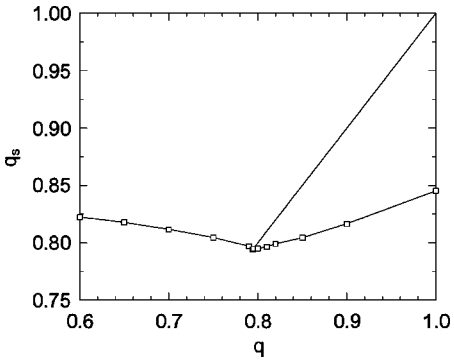

FIG. 9. Position q_s of the singularity in the stationary probability density of the extremal CP. The upper line of singularities, $x=q$, bifurcates from q_s at the critical value $q_{c,E}$.

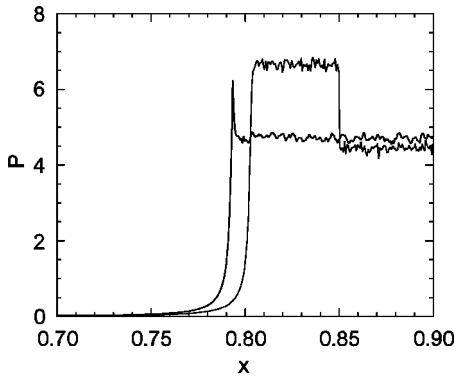

FIG. 10. Stationary probability density $\overline{p}(x)$ in the CP_E for $q=0.794$ (left) and $q=0.85$ (right); system size $L=1600$.

infinite-size limit), are shown in Fig. 9. The lower singularity q_s is seen to bifurcate from the line of singularities just at the critical point, in qualitative agreement with MFT. Note however that the position of the singularity is not constant for $q<q_{c,E}$, as predicted by MFT.

The density $\overline{p}(x)$ is shown for $q=0.794\simeq q_{c,E}$ and $q=0.85$ in Fig. 10. In the latter case it is evident that the step at $x=q$ is sharp (this is true even for small systems). Note that its position is predicted exactly by mean-field theory. All of these observations highlight the fact that the step at $x=q$ is not related to a phase transition, but derives instead from the singular nature of the updating rule, Eq. (2). This rule treats active and inactive neighbors of the central site differently. In particular, a variable x (associated with a neighbor of the central site), lying in the interval $[q,1]$ is updated to [0,1], effectively depleting the former interval, so that $p(x)$ falls suddenly at $x=q$.

The step at $x=q_s$, by contrast, is subject to finite-size rounding, and becomes sharper with increasing system size, as is characteristic of a critical singularity. The finite width of the peak at $x=q_c$ (in the process with $q=q_{c,E}$), appears to be a finite size effect as well, it becomes sharper with increasing L, suggesting that the singularities merge in the limit $L\to\infty$.

E. Anisotropic ABS model

The scaling behavior of the Bak-Sneppen model changes when the updating rule is asymmetric [29]. The same critical exponents are found for a highly anisotropic version in which at each step, only the minimal site and its neighbor on the right are updated [30], and for weak anisotropy [16,31], so that one may identify an anisotropic BS universality class. In this section we report results of spreading simulations of the anisotropic absorbing BS model. To obtain these results, we simulated the anisotropic ABS (in the highly anisotropic version) in studies extending to a maximum time of 1.6×10^5, using 3×10^5 realizations.

Analyzing the local slope $\delta(t)=d\ln P/d\ln t$, we determined the threshold of this model to be $q_{c,E}=0.723\,70(2)$. [This is a substantial improvement over the earlier estimate of 0.7240(1) [32].] A typical evolution of the critical spreading process is shown in Fig. 11. The local slope $\delta(t)$ yields the estimate $\delta=0.234(5)$. For anisotropic models we define $R^2(t)$ as the mean-square *radius of gyration*, i.e., the distance is measured relative to the current center of mass of the set of active sites, rather than to a fixed origin. This is done to eliminate a spurious contribution due simply to the overall drift in the active region. For the anisotropic ABS model $R^2(t)$ may again be fit with an expression of the form of Eq. (6), with $z_{sp}=1.425(10)$ and $\phi_R=2.3(2)$. The exponents δ and z_{sp} are quite different from those of the isotropic model. Despite these differences, we again find $\eta=0$ for the anisotropic model. As before, the mean number of active sites $n(t)$ saturates at long times, more rapidly in fact than in the isotropic ABS model (see Fig. 6, inset). We are able to fit the data well using $n(t)=n_\infty(1-e^{-ct^{1/4}})$ with parameters $n_\infty=5.206(3)$ and $c=0.348$.

The nonextremal model corresponding to the anisotropic ABS model is a two-site contact process, CP2, which is simply the CP3 with updating restricted to the central site and its neighbor on the right. We have verified that the spreading exponents of the CP2 model are those of directed percolation. (Here again, we define R^2 as the mean-square radius of gyration.) This leads to the interesting conclusion that a perturbation (asymmetric updating) that is *irrelevant* for a nonextremal model is relevant for the corresponding extremal system. (We note that, because the two sites in the CP2 are updated in the same manner, the model does not fall in the so-called anisotropic-DP class, for which bonds along different axes are present with different probabilities [33].)

IV. CONCLUSIONS

We investigate the relation between extremal dynamics, exemplified by the Bak-Sneppen model, and nonextremal models exhibiting a phase transition to an absorbing state, using general arguments, mean-field theory and simulation. The relation between the BS model and directed percolation was already suggested some time ago [4,5]. Here we clarify this connection by showing how a generic absorbing-state model can be transformed to an extremal one via the associated extremal-absorbing model. The nonextremal precursor of the BS model is a three-site contact process [24], CP3, which, like the original CP, belongs to the directed percolation universality class. The BS model and the extremal ver-

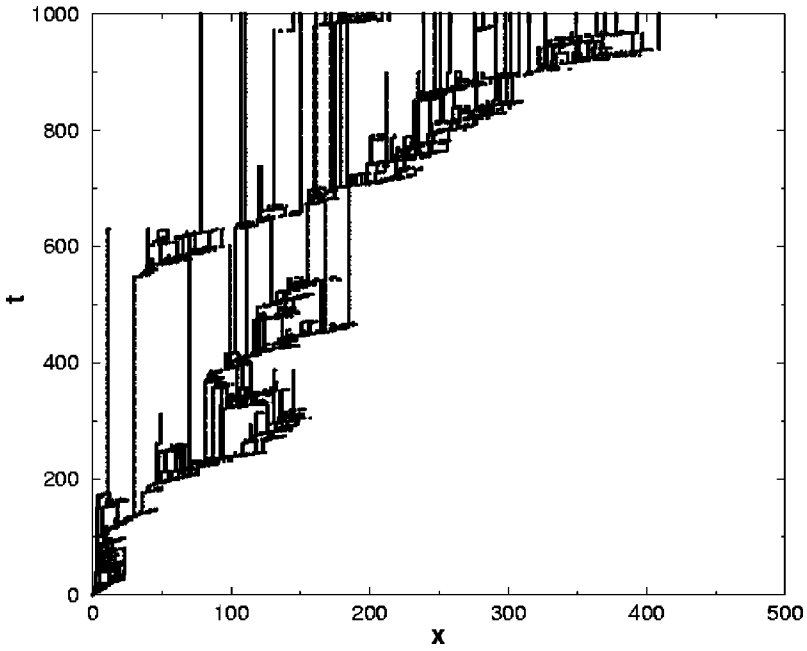

FIG. 11. Spread of activity in a typical realization of the critical anisotropic ABS model ($q = 0.723\,70$).

sion of the CP belong to a common universality class that may be dubbed extremal DP (EDP). A number of extremal dynamics classes distinct from EDP are discussed in Ref. [5]; another example is the anisotropic BS model. We expect that further extremal dynamics universality classes exist, for example, an extremal parity-conserving class [34], although examples of the latter have yet to be studied.

Our results for the critical exponents of the EDP class, which includes the BS model and the extremal CP, are compared against those of ordinary DP (in one spatial dimension) in Table I. (Here we have taken the values $\eta=0$ and $\beta=1$ to be *exact* for EDP.) The differences between the two sets of exponent values are evident. Our results $\tau=1+\delta=1.084(1)$, and $z=\nu_\parallel/\nu_\perp=2.12(1)$ are in agreement with the earlier estimates [5] of 1.07(1) and 2.10(5), respectively. Our result is however somewhat higher than Grassberger's result $\tau=1.073(3)$ [7].

Certain scaling relations are expected to hold among the critical exponents [21,23,28]. In spreading processes one expects $z_{sp}=2\nu_\perp/\nu_\parallel$; our data are nearly consistent with this, yielding $2\nu_\perp/\nu_\parallel-z_{sp}=0.022(14)$. The relation $\beta'=\delta\nu_\parallel$ is also satisfied, our data yield $\beta'-\delta\nu_\parallel=-0.013(14)$. Finally, we consider the generalized hyperscaling relation [35]

$$2\left(1+\frac{\beta}{\beta'}\right)\delta+2\eta=dz_{sp}, \tag{7}$$

in d dimensions. Using our data, we find the difference between the two sides of this relation to be 0.09(6). Our results are marred by another inconsistency that may reflect corrections to scaling or finite size effects, the product $(\beta/\nu_\perp)^{-1}(\nu_\parallel/\nu_\perp)\nu_\parallel^{-1}$, with the first two factors determined from finite-size scaling at the critical point, and the final factor obtained from the decay of the survival probability in the subcritical regime, should equal $\beta=1$; our data yield 1.08(3). These minor inconsistencies suggest that one or more of the exponents may be in error by 5% or so. Refining their values will require accumulating larger data sets in simulations of larger systems, a task we leave for future work. (The studies reported here were quite demanding computationally, representing approximately 6 months cpu time on an alpha workstation.)

In the course of our study we revisit a three-site contact process (CP3) that is the nonextremal analog of the BS model [24]. We verify that the CP3 belongs to the universality class of directed percolation, as expected [7]. We define extremal and extremal-absorbing versions of the original contact process (CP_E and CP_{EA}, respectively) and verify that their scaling properties are the same as those of the BS model. Our results confirm the relation between DP universality (in a nonextremal model) and BS universality (in the corresponding extremal model) identified some time ago by Sornette and Dornic [8]. While these authors find DP-like critical behavior in a model with parallel updating, the same behavior is also found in sequentially updated models such as the CP and CP3. The essential point is that all active sites are treated equally, unlike in extremal models, in which the currently "most active" site is updated at each step. The stationary probability density for the CP_E follows, in general terms, the predictions of mean-field theory, but certain interesting differences exist, as detailed in Sec. III E.

It is clear that when an absorbing-state model is modified to follow extremal dynamics, its critical exponents are altered. Extremal dynamics tends to slow the spread of activity in the critical and supercritical regimes. One may nevertheless inquire whether any more general features of the original model are preserved under extremalization. A candidate for such a conserved property is the critical dimension d_c. In critical phenomena, various universality classes (differing in the symmetry group of the order parameter, or the presence of conserved quantities) may share the same d_c if the algebraic structure of their continuum description (in particular, the power of the lowest-order nonlinear term in the order parameter, in a Landau-Ginzburg-Wilson effective Hamil-

tonian) is the same. Thus $d_c=4$ for all models in the n-vector family. Extending this idea to extremal models is questionable, since there is no continuum description at hand. (At first glance, the notion of extremal dynamics in a description using a *continuous* density seems problematic, since there is always one and only one extremal site.) Be that as it may, it seems plausible that if the field theory for DP [18,19,36] were somehow modified to reflect extremal dynamics, the dominant nonlinearity would not change, so that d_c would retain its value of 4, as in DP. The upper critical dimension $d_c=4$ for the BS model was established some time ago by Boettcher and Paczuski [37]. Our argument suggests that extremal versions of other absorbing-state models have the same upper critical dimension as the corresponding nonextremal model. We hope to test this prediction in future work.

Studying the anisotropic ABS model and its nonextremal counterpart, the CP2 model, we find that anisotropy is a relevant perturbation for extremal DP, while it is irrelevant for the corresponding nonextremal class. In this context we note the finding, by Dhar and Ramaswamy, that aniotropy is a relevant perturbation for the BTW sandpile [41]. The irrelevance of anisotropic updating in the CP may be understood by viewing it as a uniform drift, which can be eliminated (in the corresponding continuum description) by a Galilean transformation [42]. We suspect that other perturbations, such as diffusion, may exhibit a similar pattern of relevance.

ACKNOWLEDGMENTS

The authors are grateful to Stefano Zapperi and Jafferson Kamphorst Leal da Silva for informative discussions, and to Paulo M. C. de Oliveira for helpful comments on the paper. The authors acknowledge CNPq and FAPEMIG, Brazil, for financial support.

APPENDIX A: MEAN-FIELD THEORY

1. Extremal dynamics as a zero-temperature limit

There are several ways of formulating a mean-field theory (MFT) for extremal models. First we consider an approach [11,31] in which the probability of a site i being chosen as the central site is proportional to $e^{-\beta x_i}$; extremal dynamics is recovered in the limit $\beta\to\infty$. (In the present discussion the parameter β bears no relation to the critical exponent denoted by the same symbol in the main text.) Applied to the BS model, this approach yields the distribution $\overline{p}(x)=(3/2)\Theta(x-1/3)\Theta(1-x)$ when $\beta\to\infty$ [11,31].

In the ABS model the distribution $p(x)$ evolves via

$$\frac{\partial p(x,t)}{\partial t} = -e^{-\beta x}p(x)\Theta(q-x) + 3\int_0^q e^{-\beta y}p(y,t)dy - 2p(x,t)\int_0^q e^{-\beta y}p(y,t)dy. \tag{A1}$$

The first term represents a site with value x being selected as the central site, which is only possible if $x<q$. The second term reflects updating three sites with variables uniform on [0,1], with the integral representing the overall rate of events. The final term represents updating of the two neighboring sites, and is obtained using the mean-field factorization of the nearest-neighbor joint probability density, $p(x,y,t)\simeq p(x,t)p(y,t)$. In writing Eq. (A1) we have associated a time increment $dt=1/N$, with N the number of sites, with each event.

Equation (A1) admits an infinite set of stationary solutions for which $\overline{p}(x)=0$ on the interval $0\leqslant x\leqslant q$. These represent absorbing states. To seek an active stationary solution we let $I=\int_0^q e^{-\beta y}p(y,t)dy$, and equate the time derivative to zero, yielding

$$\overline{p}(x) = \frac{3I}{2I+\Theta(q-x)e^{-\beta x}}. \tag{A2}$$

To determine I we multiply Eq. (A2) by $e^{-\beta x}$ and integrate from $x=0$ to $x=q$, leading to $I=(e^{-\beta/3}-e^{-\beta q})/[2(1-e^{-\beta/3})]$, so that

$$\overline{p}(x) = \frac{\frac{3}{2}(e^{-\beta/3}-e^{-\beta q})}{(e^{-\beta/3}-e^{-\beta q})+\Theta(q-x)e^{-\beta x}(1-e^{-\beta/3})}. \tag{A3}$$

In the limit $\beta\to\infty$, we find, for $q>1/3$, the singular density $\overline{p}(x)=(3/2)\Theta(x-1/3)$. This is precisely the MF result for the original BS model. [When we take $\beta\to\infty$, the above expression reduces to $\overline{p}(x)=(3/2)\Theta(x-q)$ for $q<1/3$. But this density is not normalized on [0, 1] and so must be rejected. We are left with only absorbing stationary solutions for $q<1/3$.] Thus $q_{c,E}=1/3$ in the MFT of the absorbing Bak-Sneppen model. Note that the parameter q is irrelevant for $q>q_{c,E}=1/3$, as was argued in Sec. II.

A moment's reflection shows that the evolution of $p(x)$ in the (nonextremal) CP3 model is given by Eq. (A1) with $\beta=0$, since all active sites are then equally likely to be chosen as the central site. Taking the limit $\beta\to 0$ of the stationary solution, Eq. (A3), one finds, for $q\geqslant 1/3$, the stationary density

$$\overline{p}(x) = \begin{cases} \frac{1}{2}(3-q^{-1}), & x<q, \\ \frac{3}{2}, & q<x\leqslant 1. \end{cases} \tag{A4}$$

Equation (A4) confirms that the stationary density of a (nonextremal) model exhibiting an absorbing state phase transition is characterized by a steplike singularity, as asserted in Sec. II. For $q<1/3$, Eq. (A4) yields an unphysical, negative density, showing that $q_c=1/3$ for the CP3, in the mean-field approximation.

The foregoing analysis is readily extended to the extremal-absorbing contact process (CP_{EA}) defined in Sec. II. The rate of events is again given by $I=\int_0^q e^{-\beta x}p(x)dx$. At each event, there is a probability of $1/2$ that the central site (which must have $x<q$) is replaced, while with probability $1/2$ a neighbor is updated. Thus the loss terms in the equation for $p(x,t)$ are $-(1/2)[e^{-\beta x}\Theta(q-x)+I]p(x)$. The gain term corresponding to updating of the central site is simply $I/2$, but for updating a neighbor it is $(I/2)[1-P(q)+(1/q)\Theta(q-x)P(q)]$, where $P(x)=\int_0^x p(y)dy$ is the probability that a given site i has $x_i<x$. (The reason is that when updating an *active* neighbor, the variable is chosen from the

distribution uniform on $[0,q]$.) Thus the MF equation of motion is

$$\frac{\partial p}{\partial t} = -\frac{1}{2}e^{-\beta x}p(x)\Theta(q-x) + \frac{I}{2}\left(2 - P(q) + \frac{\Theta(q-x)}{q} \times P(q) - p(x)\right). \tag{A5}$$

To find the stationary solution $\overline{p}(x)$ we first note that for $0 \leqslant x < q$, setting $\partial p/\partial t$ to zero yields

$$\overline{p}(x) = AI/(I + e^{-\beta x}), \tag{A6}$$

where $A = 2 + (q^{-1} - 1)P(q)$. Integrating Eq. (A6) from $x=0$ to $x=q$, we find

$$P(q) = Aq - \frac{A}{\beta}\int_{e^{-\beta q}}^{1} \frac{du}{I+u}. \tag{A7}$$

If we now multiply Eq. (A6) by $e^{-\beta x}$ and integrate over the same interval, we obtain

$$\frac{A}{\beta}\int_{e^{-\beta q}}^{1} \frac{du}{I+u} = 1 \tag{A8}$$

leading to $P(q) = 2 - q^{-1}$ in the stationary state. We see that $q_{c,E} = 1/2$ as in the MFT of the original contact process. Evaluating the integral in Eq. (A8) one finds $I = (e^{-\beta\kappa} - e^{-\beta q})/(1 - e^{-\beta\kappa})$, where $\kappa = q^2/(3q-1)$. The stationary density is

$$\overline{p}(x) = \frac{1}{q}\frac{(e^{-\beta\kappa} - e^{-\beta q})[1 + (2 - q^{-1})\Theta(q-x)]}{(e^{-\beta\kappa} - e^{-\beta q}) + e^{-\beta x}(1 - e^{-\beta\kappa})\Theta(q-x)}. \tag{A9}$$

For $q > 1/2$, we have $\kappa < q$, and in the limit $\beta \to \infty$,

$$\overline{p}(x) = \begin{cases} 0, & x < \kappa, \\ \dfrac{1}{\kappa}, & \kappa < x < q, \\ \dfrac{1}{q}, & x > q, \end{cases} \tag{A10}$$

which is normalized and exhibits step-function singularities at $x = \kappa$ and $x = q$. For $q < 1/2$ on the other hand, $\kappa > q$ and Eq. (A9) does not yield an acceptable probability density, and we conclude that the only stationary state is the absorbing one. The critical point of the CP_{EA} thus falls at $q_{c,E} = 1/2$ in the MF approximation.

Taking $\beta \to 0$ in Eq. (A9), we obtain the probability density for the original CP,

$$\overline{p}(x) = \begin{cases} \dfrac{2q-1}{q^2}, & x < q, \\ \dfrac{1}{q}, & x > q. \end{cases} \tag{A11}$$

Finally, for the extremal CP, the equation of motion is

$$\frac{\partial p}{\partial t} = -\frac{1}{2}e^{-\beta x}p(x) + \frac{I}{2}\left(2 - P(q) + \frac{\Theta(q-x)}{q}P(q) - p(x)\right) \tag{A12}$$

with $I = \int_0^1 e^{-\beta x}p(x)dx$. To find the stationary solution we write

$$\overline{p}(x) = \frac{2 + [q^{-1}\Theta(q-x) - 1]P(q)}{1 + I^{-1}e^{-\beta x}}. \tag{A13}$$

Integrating from 0 to q and solving for $P(q)$ we find

$$P(q) = \frac{2(q-\gamma)}{q + \gamma(q^{-1} - 1)}, \tag{A14}$$

where

$$\gamma = \frac{1}{\beta}\ln\frac{I+1}{I + e^{-\beta q}}. \tag{A15}$$

Now multiply Eq. (A13) by $e^{-\beta x}$ and integrate from 0 to 1 to obtain

$$1 = A\int_0^q \frac{e^{-\beta x}dx}{I + e^{-\beta x}} + A'\int_q^1 \frac{e^{-\beta x}dx}{I + e^{-\beta x}}, \tag{A16}$$

where $A = 2/[q + \gamma(q^{-1} - 1)]$ and $A' = \gamma A/q$. If $P(q) > 0$, the first term on the right-hand side of Eq. (A16) is nonzero and dominates as $\beta \to \infty$. Equating the first term to unity then leads to $\gamma = q^2/(3q-1) = \kappa$, and then to $P(q) = 2 - q^{-1}$ which is positive for $q > 1/2$. A simple calculation then yields the distribution of Eq. (A10) in the limit $\beta \to \infty$.

If $q < 1/2$ the above solution is not valid since it implies $P(q) < 0$. We therefore take $P(q) = 0$, implying $\gamma = q$, and so $A = A' = 2$. Equation (A16) now reads

$$1 = 2q + \frac{2}{\beta}\ln\frac{I + e^{-\beta q}}{I + e^{-\beta}}. \tag{A17}$$

Solving for I and inserting the result in Eq. (A13), we find in this case $\lim_{\beta\to\infty}\overline{p}(x) = 2\Theta(x - 1/2)$. These results have been verified via numerical integration.

2. Extremal dynamics on a complete graph

Another approach to formulating MFT for the BS model considers extremal dynamics on an N-site complete graph or random-neighbor model (two neighbors are selected at random each time a site is updated); the stationary density $\overline{p}(x)$ becomes a step function in the infinite-size limit [[12,16,38–40]]. We now extend this approach to the ABS model. Let $P(x) = \mathrm{Prob}[x_i < x] = \int_0^x p(y)dy$ be the distribution function and let $Q(x) = 1 - P(x)$. By definition Q is a nonincreasing function with $Q(0) = 1$ and $Q(1) = 0$, since $p(x) = 0$ outside the interval [0,1].

Activity in the ABS model is predicated on the minimal site $x_{\min}$ being smaller than q; the probability of this event, under the MF factorization, is $1 - [Q(q)]^N$. Given $x_{\min} < q$, updating the extremal site and two neighbors results, on the average, in the increment, $dP(x) = (1/N)\{-[1 - Q(x_<)^N] - 2P(x) + 3x\}$, where $x_< \equiv \min\{x, q\}$, so that the first term represents loss of the minimal site, the second removal of two

neighbors, and the third random replacement of the three site variables with numbers uniform on [0,1]. If we adopt a time increment $dt=1/N$ for each such event, the equation of motion for P is

$$\frac{\partial P(x,t)}{\partial t} = -[1-Q(x_<,t)^N] + [1-Q(q,t)^N][3x-2P(x,t)]. \tag{A18}$$

Note that the evolution ceases if $Q(q,t)=1$, i.e., if there are no active sites. [Since Q is nonincreasing $Q(q)=1 \Rightarrow Q(x_<)=1$.]

For $q>1/3$, the stationary solution to Eq. (A18) corresponds to a density $\overline{p}(x)$ that approaches a step function, $(3/2)\Theta(x-1/3)$, as $N\to\infty$. A simple calculation yields the dominant contribution for large N,

$$\overline{Q} \simeq \begin{cases} (1-3x)^{1/N}, & x<\dfrac{1}{3}, \\ \dfrac{3}{2}(1-x)+\mathcal{O}(e^{-\text{const N}}) & x>\dfrac{1}{3}. \end{cases} \tag{A19}$$

(One should note however that the convergence is nonuniform in x, being slower the closer x is to the critical value of 1/3.) For $q<1/3$ we are unable to find an acceptable stationary solution with $Q<1$ (i.e., $\overline{p}>0$), for $x<q$, and conclude that only absorbing solutions exist.

The analysis of the ABS model on a complete graph confirms that in the infinite-size limit, the model enjoys the usual properties of the BS model for $q>q_{c,E}=1/3$, and falls into the absorbing state for $q<1/3$.

The evolution of $P(x,t)$ in the extremal CP follows, in MF approximation, the equation

$$\frac{\partial P(x,t)}{\partial t} = -\frac{1}{2}[1-Q(x,t)^N] + \frac{x}{2} - \frac{1}{2}P(x,t) + \frac{1}{2}[x^* P(q,t) + xQ(p,t)], \tag{A20}$$

where $x^*=\min\{x/q,1\}$. Numerical integration shows that the solution converges, for large N, to a stationary distribution consistent with the singular density found above in the limit $\beta\to\infty$.

APPENDIX B: SIMULATION METHOD FOR EXTREMAL DYNAMICS

We have devised an improved simulation algorithm for extremal dynamics models. Since the site with the smallest variable, $x_{\min}$, must be identified at each step, it becomes important to devise an effective search strategy. An efficient general-purpose search algorithm uses a binary tree structure to identify $x_{\min}$. One approach [7] utilizes a lattice of 2^n sites. At the first level of selection, each site is compared with one of its neighbors and the minimum of the pair selected. At the next level the minimum between each neighboring pair is selected, and so on, so that at the nth level the global minimum is identified.

A second binary scheme [26] is formulated as follows. Site 0 is placed at the apex of the tree. Site 1 is placed on the level below the apex, to the left of 0 if $x_1<x_0$, to the right if $x_1>x_0$. A site i is added to the tree in the following way: we go down the tree comparing x_i with the variables $x_1,\ldots,x_{i-1}$, turning left or right depending on whether x_i is smaller or larger than x_j, until we find an empty site. Building the tree in this way, $x_{\min}$ will occupy the leftmost position in the tree. In these schemes, maintaining the tree structure, once constructed from the initial set of variables x_i, requires a small number of operations at each step, and is many times more efficient than a repeated global search for the minimim. We find, nonetheless, that a suitably *restricted* search requires less cpu time in the stationary state.

A special property of the BS model (shared by its absorbing version, and by other extremal models), is that the minimal site falls, with a probability approaching unity as the system size grows, in the interval $[0,q_{c,E}]$. At the same time the density of sites with values in this interval approaches zero as $N\to\infty$. This suggests maintaining a list of sites having $x<q_{c,E}$ [27]. Then the search for $x_{\min}$ may be restricted to the list, except for the rare instances in which the latter is empty. (For the ABS we must in any case restrict the search to sites with $x\leqslant q$.) If the system is large, so that the typical number of sites with $x<q$ is not small, it becomes advantageous to introduce a *second* list, of sites having $x<q^{**}<q_{c,E}$. When this relatively short list is nonempty (as is usually the case) the search for $x_{\min}$ is restricted to it. In studies of the BS model, we obtained the greatest efficiency using $q^{**}=0.54$, while the criterion for the first list was $x<0.65$, that is, slightly *below* $q_{c,E}$. (The occasional need to perform a global search, in the rare instances when both lists are empty, is more than compensated by their reduced sizes when using these values.) Compared with the binary tree method, our approach results in threefold reduction in CPU time, in the stationary state, for a system of 1000 sites. (The binary tree approach may prove more efficient for studying transients, since initially the lists will not be short, if the x_i values are chosen uniformly on [0,1].)

[1] P. Bak and K. Sneppen, Phys. Rev. Lett. **71**, 4083 (1993).
[2] K. Sneppen, Phys. Rev. Lett. **69**, 3539 (1992).
[3] H. Leschhorn and L.-H. Tang Phys. Rev. E **49**, 1238 (1994).
[4] M. Paczuski, S. Maslov, and P. Bak, Europhys. Lett. **27**, 97 (1994).
[5] M. Paczuski, S. Maslov, and P. Bak, Phys. Rev. E **53**, 414 (1996).
[6] D. Sornette, A. Johansen, and I. Dornic, J. Phys. I **5**, 325 (1995).
[7] P. Grassberger, Phys. Lett. A **200**, 277 (1995).
[8] D. Sornette and I. Dornic, Phys. Rev. E **54**, 3334 (1996).
[9] P. Grassberger and Y. C. Zhang, Physica A **224**, 169 (1996).

[10] P. Bak, C. Tang, and K. Wiesenfeld, Phys. Rev. Lett. **59**, 381 (1987).
[11] R. Dickman, M. A. Muñoz, A. Vespignani, and S. Zapperi, Braz. J. Phys. **30**, 27 (2000).
[12] H. Flyvbjerg, K. Sneppen, and P. Bak, Phys. Rev. Lett. **71**, 4087 (1993).
[13] B. Drossel, Adv. Phys. **50**, 209 (2001).
[14] T. E. Harris, Ann. Prob. **2**, 969 (1974).
[15] G. J. M. Garcia and R. Dickman, Physica A **332**, 318 (2004).
[16] G. J. M. Garcia and R. Dickman, Physica A **342**, 516 (2004).
[17] D. A. Head and G. J. Rodgers, J. Phys. A **31**, 3977 (1998).
[18] H. K. Janssen, Z. Phys. B: Condens. Matter **42**, 151 (1981).
[19] P. Grassberger, Z. Phys. B: Condens. Matter **47**, 365 (1982).
[20] T. M. Liggett, *Interacting Particle Systems* (Springer-Verlag, New York, 1985).
[21] H. Hinrichsen, Adv. Phys. **49**, 815 (2000).
[22] N. Konno, *Phase Transitions of Interacting Particle Systems* (World Scientific, Singapore, 1994).
[23] J. Marro and R. Dickman, *Nonequilibrium Phase Transitions in Lattice Models* (Cambridge University Press, Cambridge, 1999).
[24] B. Jovanović, S. V. Buldyrev, S. Havlin, and H. E. Stanley, Phys. Rev. E **50**, R2403 (1994).
[25] M. Paczuski, P. Bak, and S. Maslov, Phys. Rev. Lett. **74**, 4253 (1995).
[26] P. M. C. de Oliveira (private communication). J. S. Sá Martins and P. M. C. de Oliveira, Braz. J. Phys. **34**, 1077 (2004).
[27] The idea of using a single list, of sites with $x<0.668$ (i.e., below a value slightly above the threshold), is already suggested in Ref. [26].
[28] P. Grassberger and A. de la Torre, Ann. Phys. (N.Y.) **122**, 373 (1979).
[29] M. Vendruscolo, P. De Los Rios, and L. Bonesi Phys. Rev. E **54**, 6053 (1996).
[30] S. Maslov, P. De Los Rios, M. Marsili, and Y.-C. Zhang, Phys. Rev. E **58**, 7141 (1998).
[31] D. Head, Eur. Phys. J. B **17**, 289 (2000).
[32] G. J. M. Garcia and R. Dickman, Physica A **342**, 164 (2004).
[33] See J. Kamphorst Leal da Silva and M. Droz, J. Phys. C **18**, 745 (1985), and references therein.
[34] P. Grassberger, F. Krause, and T. von der Twer, J. Phys. A **17**, L105 (1984);P. Grassberger, *ibid.* **22**, L1103 (1989);H. Takayasu and A. Yu. Tretyakov, Phys. Rev. Lett. **68**, 3060 (1992);I. Jensen, Phys. Rev. E **50**, 3623 (1994).
[35] J. F. F. Mendes, R. Dickman, M. Henkel, and M. C. Marques, J. Phys. A **27**, 3019 (1994).
[36] J. L. Cardy and R. L. Sugar, J. Phys. A **13**, L423 (1980).
[37] S. Boettcher and M. Paczuski, Phys. Rev. Lett. **84**, 2267 (2000).
[38] J. de Boer, B. Derrida, H. Flyvbjerg, A. D. Jackson, and T. Wettig, Phys. Rev. Lett. **73**, 906 (1994).
[39] J. de Boer, A. D. Jackson, and T. Wettig, Phys. Rev. E **51**, 1059 (1995).
[40] I. Jensen, J. Phys. A **29**, 7013 (1996).
[41] D. Dhar and R. Ramaswamy, Phys. Rev. Lett. **63**, 1659 (1989).
[42] S.-C. Park and H. Park, Phys. Rev. Lett. **94**, 065701 (2005).